Effects of Pyrolysis Conditions on Physicochemical Properties of Oat Hull Derived Biochar

María Eugenia González,[a,*] Luis Romero-Hermoso,[b] Aixa González,[a] Pamela Hidalgo,[b] Sebastian Meier,[b,c] Rodrigo Navia,[b,d,e] and Mara Cea [b,d]

The effects of the pyrolysis conditions in terms of temperature (400 to 600 °C), residence time (0.5 to 3.5 h), nitrogen flux (0 to 1 L/min), and temperature increase rate (1.5 to 3 °C/min) on the physicochemical properties of biochar were studied. The physicochemical properties evaluated in the biochar were specific surface area, pore volume, average pore size, total carbon content, pH, total acidity, elemental composition, and polycyclic aromatic hydrocarbons (PAHs) content. A higher specific surface area of 108.28 m^2/g and a mean pore size diameter of about 2.24 nm were found when the pyrolysis was conducted at 600 °C. In general, the pH and total acidity increased with the increased pyrolysis temperature. The total PAH concentration in all of the combinations studied varied from 0.16 to 8.73 µg/kg, and only phenanthrene, pyrene, and chrysene were detected. The increased temperature seemed to decrease the PAH concentration in the biochar. Nevertheless, there was no correlation found between the PAH content and the combined evaluated parameters.

Keywords: Pyrolysis conditions; Biochar; Physicochemical properties; Polycyclic aromatic hydrocarbons

*Contact information: a: Núcleo de Investigación en Bioproductos y Materiales Avanzados (BioMA), Dirección de Investigación, Universidad Católica de Temuco, Temuco, Chile; b: Scientific and Technological Bio Resources Nucleus-BIOREN, University of La Frontera, Av. Francisco Salazar 01145, Temuco, Chile; c: Instituto Nacional de Investigaciones Agropecuarias. INIA Carillanca, Casilla Postal 58-D Temuco, Chile; d: Department of Chemical Engineering, University of La Frontera, Av. Francisco Salazar 01145, Temuco, Chile; e: Centre for Biotechnology & Bioengineering (CeBiB), University of La Frontera, Av. Francisco Salazar 01145, Temuco, Chile; * Corresponding author: mgonzalez@uct.cl*

INTRODUCTION

In recent years, the number of biochar publications has increased rapidly, with a number of studies evaluating the physical and chemical characteristics of biochar used as a soil amendment (Novak *et al.* 2009; Biederman and Harpole 2013), soil remediator (Qin *et al.* 2013; Waqas *et al.* 2014), raw material for catalyst development (Dehkhoda and Ellis 2013), modifier agent in the controlled release formulations of nutrients (González *et al.* 2015), and immobilization support (González *et al.* 2013).

The physicochemical properties of biochar, such as pore diameter, size distribution, total surface area, and nutrient content, are closely related to the pyrolysis conditions and the original biomass feedstock (Chen *et al.* 2014; Manyà *et al.* 2014). The pyrolysis temperature causes chemical and physical changes to the feedstock, such as decreasing the H/C, O/C, and (N+O)/C ratios. For example, high temperatures increase the specific surface area (Devi and Saroha 2015) but decrease the amount of biochar produced, and they cause demethylation and decarboxylation reactions that result in high amounts of carbonized and aromatic structures (Chen *et al.* 2014; Devi and Saroha 2015).

If the pyrolysis temperature is too high, then there is an excessive amount of carbon volatilization, and low concentrations of functional groups are obtained (Chen *et al.* 2014). The chemical composition, pH, surface charge, and thermal stability of biochar are also affected by the pyrolysis temperature, and these properties influence the degree of biochar reactivity (Downie *et al.* 2009; Chen *et al.* 2014).

Additionally, the operational pyrolysis conditions can lead to the production of polycyclic aromatic hydrocarbons (PAHs), which are strongly adsorbed by the biochar (Khan *et al.* 2013; Yargicoglu *et al.* 2015). The presence of PAHs in biochar is a matter of concern because of their potential carcinogenic and mutagenic characteristics (Anjum *et al.* 2014; Devi and Saroha 2015). Thus, the amount of these toxic constituents in the biochar determines the potential use of the material. For instance, before agricultural soil application, it is necessary to test the PAHs content in the biochars for their potential genotoxicity and risk of contamination (Hilber *et al.* 2012; Anjum *et al.* 2014).

There are few studies on the interaction between the pyrolysis conditions and biochar quality, and in particular, the PAHs content. Currently, the principal reports addressing the effect of pyrolysis temperature, residence time, and raw material on the PAHs content are by Hale *et al.* (2012), Keiluweit *et al.* (2012), Devi and Saroha (2015), and Fu *et al.* (2016). However, these parameters have been studied separately or not systematically. Only Buss *et al.* (2016) reported the effect of the residence time, highest treatment temperature (HTT), and carrier gas flow rate on the total concentrations of 16 US EPA PAHs in biochar. However, there is no known correlation between the biochar physicochemical properties, PAHs content, and pyrolysis conditions.

The aim of this study was to evaluate the effect of temperature, residence time, nitrogen flux, and temperature increase rate on the oat hull derived biochar yield, its physicochemical properties, and PAHs formation and accumulation.

EXPERIMENTAL

Material and Methods

Experimental design

An unreplicated 2-level factorial design was adopted to evaluate the effects of the four main factors, temperature (T), residence time (t_R), nitrogen flux (f_N), and temperature increase rate (T_i), on the physicochemical properties of the oat hull derived biochar. The computational program Design Expert 6.0 (Stat-Ease, Inc., Minneapolis, MN, USA) was used to generate the experimental design and to perform the appropriate statistical analyses. To estimate the intrinsic experimental error and the overall curvature effect simultaneously, four replicates at the center point were carried out. In this method, each parameter was coded to a -1, 0, or +1 interval, according to its range. The low, middle, and high levels of the parameter corresponded to -1, 0, and +1, respectively. Based upon these coded factors, the list of experiments required for the study with four parameters is shown in Table 1.

The following response variables were evaluated: specific surface area (BET) (Y_{BET}), carbon content (Y_C), pore volume (Y_{Pv}), average pore size diameter (BJH) (Y_{Pd}), pH (Y_{pH}), and total acidity (Y_{TA}).

Table 1. Matrix of the 2^4 Factorial Design Adopted in the Biochar Production Trials

Level		Factors			
		X_1 Temperature (ºC)	X_2 Residence time (h)	X_3 Nitrogen Flux (L/min)	X_4 Temperature increase rate (ºC/ min)
Low (-1)		400	0.5	0.0	1.5
Middle (0)		500	2.0	0.5	2.25
High (+1)		600	3.5	1.0	3.0
Run	**Identification Sample**	**Factors**			
		X_1	X_2	X_3	X_4
1	BC1	1	-1	-1	1
2	BC2	0	0	0	0
3	BC3	1	1	-1	-1
4	BC4	-1	-1	-1	-1
5	BC5	0	0	0	0
6	BC6	-1	-1	1	1
7	BC7	1	1	1	1
8	BC8	-1	1	-1	1
9	BC9	1	-1	1	-1
10	BC10	0	0	0	0
11	BC11	-1	-1	1	1
12	BC12	0	0	0	0

Biochar Production

Oat hull was used as the raw material to obtain the biochar. The chemical characterization of this raw material was described previously (González *et al.* 2013). It was found that the total carbon (C_T) is 42.65%, total nitrogen (N_T) is 0.49%, H, O, and S contents were 4.72%, 69.72%, and 0.96%, respectively. The ash content is 6.20%, and pH is 3.06. The lignin, cellulose, and hemicellulose contents are 7.5%, 34.3%, and 26%, respectively.

The oat hull derived biochar was produced at the Center of Waste Management and Bioenergy, Universidad de La Frontera, Chile. For each experimental run given by the factorial design (Table 1), the pyrolyzer was fed 500 g of raw material and then purged with nitrogen gas to displace the air before starting the process.

Once the pyrolysis process was concluded, the liquid fraction (bio-oil) and biochar were then weighed to determine their respective yields. The gas yield was estimated from the overall mass balance.

Biochar Characterization

A number of physicochemical properties of the biochar were determined. The pH (1/10, wt/v) was measured electrochemically with a pH meter (Thermo Orion 9512, Waltham, MA, USA) according to Chen *et al.* (2014). The total N, C, H, and S contents were measured using a CHNS-O (Eurovector EA 3000, Changsha, China). The total acidity ($Ba(OH)_2$ method) and carboxylic acidity ($Ca(C_2H_3O_2)_2$ method) were determined according to Tan (1996). The phenolic acidity was determined by the difference between the total and carboxylic acidities. The isoelectric points (IP) and Z potential were determined using a Zetasizer Nano ZS (Malvern Co., Malvern, UK) coupled with a MPT-2 autotitrator. The samples were dispersed in deionized water at 25 °C and titrated with 1 M HCl and 1 M NaOH (Qiu and Ling 2006).

The surface functional groups of the biochar were characterized by Fourier transform infrared spectroscopy (FTIR) using a Bruker Tensor 27 spectrometer (Karlsruhe, Germany). The sample discs were prepared by mixing the oven-dried samples (at 105 °C) with spectroscopic-grade KBr at ambient temperature in a biochar/KBr ratio of 1:200. The FTIR spectra were recorded at 32 scans with a resolution of 4 cm^{-1} from wavenumbers 4000 to 500 cm^{-1} (González *et al.* 2013).

The specific surface area (Brunauer-Emmett-Teller), pore volume (BJH), and average pore size diameter were determined using a NOVA 1000e porosimeter (Quantachrome, Boynton Beach, FL, USA) by adsorbing and desorbing nitrogen at 77 K on the samples that were previously dried and outgassed at 160 °C for 16 h (González *et al.* 2013).

The scanning electron micrographs (SEM) were recorded by scanning electron microscopy variable pressure (VP-SEM) to analyse the structure and chemical contrast with a SU-3500 Microscope (Hitachi-Japan, Hitachinaka, Japan). The biochar samples were mounted on a 12 mm aluminium sample holder (stub) using carbon double-sided tape for adhesion.

Extraction and Quantification of Polycyclic Aromatic Hydrocarbons (PAHs) Concentration in Biochar

The PAHs concentration in the biochar and raw oat hull material was determined by gas chromatography coupled with mass spectrometry (GC-MS) after Soxhlet extraction. The Soxhlet extraction was carried out according to the methodology described by Hale *et al.* (2012) using toluene as the extractant, and the PAHs were quantified through the US EPA method TO-13A (1999). The toluene of each sample was evaporated using N_2 gas and suspension in n-hexane (200 μL) mixed with 2 μL of deuterated acenaphthene-d10, phenanthrene-d10, chrysene-d12, and perylene-d12, which were used as internal standards, for the PAHs quantification.

Then, the samples were cleaned by passing them through a silica gel column and eluted with 10 mL of a mixture of dichloromethane/n-hexane. Finally, the samples were analyzed by GC/MS on a QP2010 plus (Shimadzu, Tokyo, Japan). The PAHs separation was accomplished by using a capillary column (30 m x 0.32 mm x 0.25 μm film thickness RTX-5MS, Restek, Bellefonte, PA, USA) with helium as the carrier gas and a temperature program which started at 70 °C for 4 min, then the temperature increased to 300 °C at a rate of 10 °C/min, and the temperature remained at 300 °C for 10 min. The total temperature program time was 37 min.

RESULTS AND DISCUSSION

The pyrolysis results under the different operational conditions are summarized in Table 2. For each response, the program delivered a regression model, which included the linear and interaction terms. Thus, the functional relationships between the response (y) and coded independent variables (x_1 for temperature, x_2 for residence time, x_3 for nitrogen flow, and x_4 for temperature increase rate) were quantified by means of the estimated parameters of the regression model.

Table 2. Experimental Results Obtained from the Factorial Design

Run	Identification Sample	Y_{BET} (m^2/g)	Y_C (%)	Y_{Vp} (cc/g)	Y_{Pd} (nm)
1	BC1	33.9	78.27	0.016	1.48
2	BC2	11.7	73.91	0.015	2.14
3	BC3	101.1	79.20	0.019	1.29
4	BC4	1.3	69.13	0.0011	1.48
5	BC5	13.1	77.35	0.014	1.66
6	BC6	13.4	69.35	0.0032	2.22
7	BC7	120.5	79.67	0.019	1.02
8	BC8	15.2	69.81	0.0038	2.24
9	BC9	58.6	79.89	0.007	1.29
10	BC10	10.9	73.35	0.012	1.73
11	BC11	0.90	68.62	*	*
12	BC12	9.57	71.67	0.015	1.80

*The BJH model was unable to calculate the pore volumen and pore size distribution

The model for the specific surface area (Y_{BET}, m^2/g), after performing 12 experiments and discarding the insignificant effects, was derived from the following

equation,

$$Y_{BET} = 43.1125 + 35.4125A - 476.925B + 19.437C + 476.437ACD \quad (1)$$

where A, B, C, and D are the coded factors of temperature (°C), temperature increase rate (°C/min), residence time (h), and nitrogen flux (L/min), respectively. The coded factors were determined according to the following equations,

$$A = -1 + (T - 400) / 100 \quad (2)$$

$$B = -1 + (Ti - 1.5) / 0.75 \quad (3)$$

$$C = -1 + (Rt - 0.5) / 1.5 \quad (4)$$

$$D = -1 + (Nf - 0) / 0.5 \quad (5)$$

The model for the average pore size diameter (Y_{Pd}, nm), after discarding the insignificant effects, is given by Eq. (6),

$$Y_{Pd} = 1.3775 + 0.315C \quad (6)$$

In the case of the carbon content (Y_C), pore volume (Y_{Vp}), pH (Y_{pH}), and total acidity (Y_{TA}), the experimental results were not adjusted to the mathematical model, and that was reflected in the low R^2 values obtained (Table 3).

Table 3. Results of Test of Significance of Factors and Interaction for the Models

Factors or Interactions	*p*-Value of Y_{BET} Factors	*p*-Value of Y_C Factors	*p*-Value of Y_{Vp} Factors	*p*-Value of Y_{Pd} Factors
A	< 0.0001	0.0095	0.0009	0.2484
B	< 0.0001	0.9134	0.0085	0.0397
C	< 0.0001	0.7739	0.0136	< 0.0001
D	0.0021	0.8787	0.0754	0.0473
AB	0.2073	0.8808	0.0981	0.1057
AC	0.0001	0.9239	0.1074	0.0106
AD	0.0016	0.6809	0.1655	0.1825
ACD	< 0.0001	0.9185	0.0088	0.0371
Model	< 0.0001	0.1226	0.1076	< 0.0001
R^2	0.9996	-	-	0.9677

Effect of Pyrolysis Process Conditions on the Specific Surface Area (BET) and Average Pore Size Diameter of Biochar

As shown in Fig. 1a, the specific surface area increased with higher temperatures and residence times. The temperature was the most significant variable that affected the results. In particular, the specific surface area was strongly affected, which became higher with higher temperatures (Yao *et al.* 2012; Park *et al.* 2013; Devi and Saroha 2015). The effect of the residence time was demonstrated by Klasson *et al.* (2014), which showed that increasing the residence time from 120 to 240 min in the pyrolysis process carried out at 800 °C increased the specific surface area from 44 to 423 m^2/g in the almond shell derived biochar. In this study, the interaction between the temperature and residence time favored the production of biochar with higher specific surface areas. For example, a specific surface area of 120.5 m^2/g was obtained at 600 °C and 210 min residence time, which was much higher compared to the specific surface area of 33.9 m^2/g that was obtained at the

same temperature and 30 min residence time (Table 2). However, the temperature had a larger effect on the specific surface area of the biochar than the residence time, which is reflected in the inclination of the level curve obtained for the temperature (Fig. 1a).

The specific surface area during pyrolysis was not only dependent on the temperature and residence time, but also depended on the characteristics of the raw material (Klasson *et al.* 2014). For instance, woody biomass often has higher cellulose, hemicellulose, and lignin contents compared to biomass from herbaceous or grass species, and the proportion of each compound can influence the biochar surface characteristics, such as surface area, surface acidity, pH, functional groups, and other properties (Keiluweit *et al.* 2010; González *et al.* 2013). A high lignin content combined with high temperatures leads to high specific surface areas (Li *et al.* 2014). Therefore, due to the low lignin content of oat hull (8%), it was expected that the biochar would have a low specific surface area compared to other raw materials that underwent similar pyrolysis conditions, such as the biochar obtained by Li *et al.* (2014) from pyrolyzed lignin, cellulose, and wood. However, the obtainable by-products from oat hull residue were very low or null, therefore, the biochar from oat hull is of great interest in order to obtain a cost effective sorbent for heavy metal removal from contaminated water and soils.

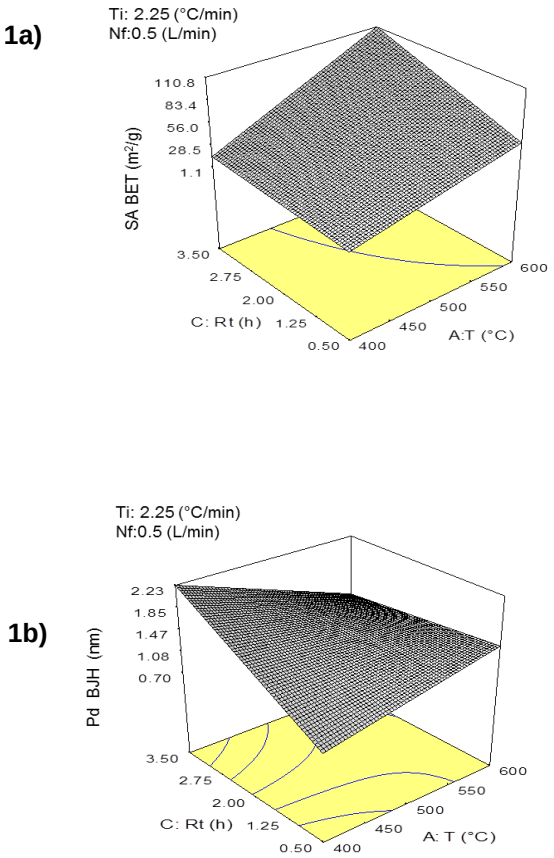

Fig. 1. a) Three-dimensional graph of the specific surface area model with the effects of temperature and residence time on the specific surface area (BET) ($P < 0.05$) (at T_i = 2.25 °C/min and f_N = 0.50 L/min). b) three-dimensional graph of the average pore size diameter (BJH) model with the effects of the temperature and residence time on the average pore size diameter (BJH) ($P < 0.05$) (at T_i = 2.25 °C/min and f_N = 0.50 L/min).

Figure 1b shows the effect of the residence time and pyrolysis temperature on the average pore size diameter of the biochar. For this property, the residence time was shown to have the most significant effect compared to the temperature. In this sense, the increased residence times and low temperatures produced a biochar having pore size diameters in the range of mesopores (between 2 nm and 50 nm). The opposite effect was observed in Fig. 1b, where high temperatures (~ 600 °C) and high residence times allowed for completed reactions, which led to higher degrees of order in the biochar structure and pores with smaller diameters (< 2nm) or micropores (Downie *et al.* 2009). It is necessary to consider that mesopores are crucial to the liquid-solid adsorption processes in soils (Downie *et al.* 2009). In addition, biochar with larger pore sizes can be used by soil microorganisms as protection (Thies and Rilling 2009).

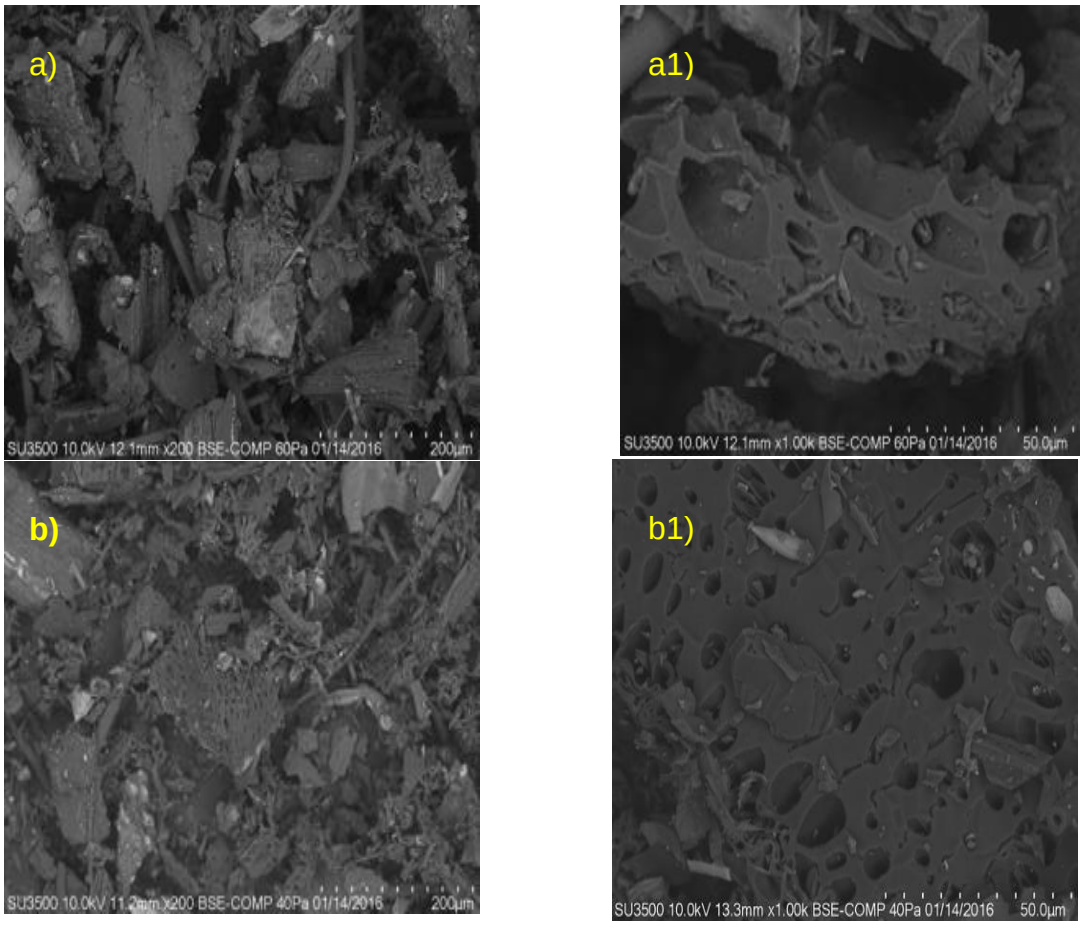

Fig. 2. SEMs of (a and a1) oat hull biochar pyrolyzed at T = 400 ºC, T_i = 3.0 ºC/min, t_R = 3.5 h, and f_N = 0.0 L/min at different scales (BC8) and (b and b1) oat hull biochar pyrolyzed at T = 600ºC, T_i = 3.0 ºC/min, t_R = 3.5 h, and f_N=1.0 L/min (BC7) at different scales.

The average pore size diameter of the biochar was influenced by the nature of the biomass and pyrolysis conditions. The average pore size diameter of the biochar also has implications for determining the suitability of this product for specific applications, such as an adsorbent, support material, and other applications (Downie *et al.* 2009). The SEM images show that the biochar had a heterogeneous structure with differences in the porous structure that were due mainly to the different treatments that were applied (Fig. 2).

Several reports described that increasing the heating rates determines the extent of pore formation. In fact, Cetin *et al*. (2004) found that the biochars generated under atmospheric pressure and low heating rates generated a product that consisted mainly of micropores, whereas those prepared at high heating rates contained a high amount of macropores. This was a result of melting processes. However, in this study there was no effect of increasing heating rate on the pore size from, due to the short range evaluated.

The optimized mathematical models used to obtain the high values of specific surface area and average pore size diameter had the following parameters: T of 599.83 °C, T_i of 2.94 °C/min, t_R of 3.40 h, and f_N of 1.0 L/min, and T of 600 °C, T_i of 2.96 °C/min, t_R of 3.5 h, and f_N of 0.89 L/min, respectively (Table 4).

These models were further validated through the experiments performed at these operating conditions (Table 4). The difference between the experimental data and mathematical model for the specific surface area was less than 11%, and for the average pore size diameter, there was a less than 5% difference. As was expected, the operational conditions to maximize the specific surface area and average pore size diameter were similar for both properties, and a relationship between the total specific surface area and average pore size diameter was determined. The increase in the pyrolysis temperature allowed for more structured surfaces and pores with smaller diameter.

The biochar produced at high temperatures, where the micropores are the main contributor to the higher values of specific surface area, are adequate to be used as adsorbent for small molecules, gases, and common solvents (Downie *et al*. 2009).

Table 4. Predicted and Experimental Values for the Specific Surface Area and Average Pore Size Diameter of Biochar

Parameters	Predicted by Models	Observed Value
Specific surface area (BET) (m^2/g)	120.51	108.28
Average pore size diameter BJH (nm)	2.36	2.24

The specific surface area model was pyrolyzed at T= 599.83 °C, T_i = 2.94 °C/min, t_R = 3.40 h, and f_N = 1 L/min, and the average pore size diameter model was pyrolyzed at T = 600ºC, T_i = 2.96 °C/min, t_R =3.5 h, and f_N = 0.89 L/min.

Effect of Pyrolysis Process Conditions on Product Yields

The lower pyrolysis temperatures produced high yields of biochar, while the biochar yield rapidly decreased with increasing pyrolysis temperature (Table 5). This reduction with increasing pyrolysis temperatures has been reported to be mainly due to thermal degradation of cellulose and hemicellulose as well as dehydration of hydroxyl groups (Demirbas 2004). At temperatures greater than 300 °C, cellulose becomes depolymerized, which produces volatile compounds (Lehmann and Joseph 2009). Even though the heating rate and residence (Demirbas 2004) affect the biochar yield, in this study, at increasing heating rates, no important differences in the biochar yield were observed.

Table 5. Pyrolysis Products Yield of the Different Experimental Runs from the Factorial Design

Pyrolysis Conditions				Biomass (g)	Yield (%)		
T (°C)	T_i (°C/min)	t_R (h)	f_N (L/min)		Biochar	Bio-oil	Syngas
600	3.0	0.5	0.0	500	34.89	45.83	19.28
500	2.25	2.0	0.5	500	40.60	37.50	21.90
600	1.5	3.5	0.0	500	31.90	43.94	24.17
400	1.5	0.5	0.0	500	49.57	38.31	20.82
500	2.25	2.0	0.5	500	44.43	43.58	15.98
400	1.5	3.5	1.0	500	49.49	37.26	12.23
600	3.0	3.5	1.0	500	32.70	40.64	26.66
400	3.0	3.5	0.0	500	46.30	28.91	24.78
600	1.5	0.5	1.0	500	30.46	46.43	19.12
500	2.25	2.0	0.5	500	45.72	37.92	25.06
400	3.0	0.5	1.0	500	49.89	36.90	12.99
500	2.3	2.0	0.5	500	45.43	44.64	9.92

Effect of Pyrolysis Process Conditions on PAHs Concentration

The principal PAHs detected were phenanthrene, pyrene, and chrysene (Table 6), which are included in the 16 PAHs classified by the US EPA as priority-pollutants based on their toxicity to humans and frequency of occurrence in hazardous waste sites (ATSDR 2005). In addition, based on the number of benzene rings, these compounds have been classified into three categories: i) high molecular mass PAHs with five and six rings, which are benzo[b]fluoranthene, benzo[k]fluoranthene, benzo[a]pyrene, indeno[1,2,3-cd]pyrene, dibenz[a,h]antracene, and benzo[ghi]perylene (BbF, BkF, BaP, IND, DAB, and Bghip, respectively), ii) middle molecular mass PAHs with four rings, which are fluoranthene, pyrene, benz[a]anthracene, and chrysene (Fla, Pyr, BaA, and CHR, respectively), and iii) low molecular mass PAHs with two and three rings, which are naphthalene, acenaphthylene, acenaphthene, fluorine, phenanthrene, and anthracene (Nap, Acpy, Acp, Flu, Phe, and Ant, respectively) (Hu *et al.* 2014). In the raw material, PAHs were not detected, and in the biochar samples, the total PAHs concentration varied from 0.16 to 8.73 μg/kg (Fig. 3).

The highest concentration of the total PAHs for this study was found in the biochar produced at 400 °C (BC4) (Fig. 3). The present results are consistent with the studies reported by Devi and Saroha (2015) and Alburquerque *et al.* (2015) for biochar produced from paper mill effluent treatment plant sludge and pinewood. Two of the predominant compounds detected in the present study (phenanthrene and pyrene) also were observed by the mentioned researchers, who used pyrolysis temperatures between 350 and 550 °C. Moreover, Devi and Saroha (2015) and Alburquerque *et al.* (2015) reported a decreasing PAHs concentration when the temperature increased, similar to our results. Buss *et al.* (2016) collected and analyzed 46 biochar produced under different operational conditions and different configuration of reactors and concluded that feedstock characteristics highly influenced on PAH concentrations. Also, it was found that the conversion technology is a factor to be considered. Regarding the temperature, Buss *et al.* (2016), after analyzing the samples, were unable to recommend a particular pyrolysis temperature for the production of biochar with low PAH content.

Table 6. Concentration of PAHs in Biochars Pyrolyzed at Different Operational Conditions

Parameter	Biochar Samples											
	BC1	**BC2**	**BC3**	**BC4**	**BC5**	**BC6**	**BC7**	**BC8**	**BC9**	**BC10**	**BC11**	**BC12**
pH	10.82	10.60	10.63	8.11	10.86	10.24	10.88	9.76	10.77	10.64	8.56	10.43
S_{TA} (mmol/g)	11.1	12.8	12.8	15.3	13.2	12.2	13.7	12.3	13.4	11.3	12.4	13.3
S_{COOH} (mmol/g)	n.d	n.d	n.d	n.d	n.d	n.d	n.d	n.d	n.d	n.d	n.d	n.d
S_{OH} (mmol/g)	11.1	12.8	12.8	15.3	13.2	12.2	13.7	12.3	13.4	11.3	12.4	13.3
IP	2.86	1.67	1.74	1.72	1.56	1.20	2.21	1.90	1.85	1.76	1.89	1.55
C (%)	78.27	73.91	79.20	69.13	77.35	69.35	79.67	69.81	79.89	73.35	68.62	71.67
N (%)	4.68	5.13	5.36	5.77	6.51	6.39	7.37	7.72	8.22	7.21	5.83	6.29
H (%)	1.97	2.47	1.65	3.44	2.86	3.21	1.84	3.29	2.15	2.46	3.78	2.46
S (%)	n.d	n.d	n.d	n.d	n.d	n.d	n.d	n.d	n.d	n.d	n.d	n.d

Note: n.d indicates not detected. Naphthalene (Nap), Acenaphthylene (Acpy), Acenaphthene (Acp), Fluorene (Flu), Fluoranthene (Fla), Anthracene (Ant), Benz[a]anthracene (BaA), Benzo[b]fluoranthen (BbF), Benzo[k]fluorane (BkF), Benzo[a]pyrene (BaP), Indeno[1,2,3-cd]pyre (IND), Dibenz[a,h]anthracene (DBA), and Benzo[ghi]perylene (Bghip) were measured, but these compounds were not detected.

Table 7. Chemical Properties of Biochar Samples Pyrolyzed at Different Conditions

PAHs (µg/kg)	Oat hull	BC1	BC2	BC3	BC4	BC5	BC6	BC7	BC8	BC9	BC10	BC11	BC12
Phenanthrene (Phe)	n.d	0.44	4.53	2.18	5.27	0.53	n.d	0.87	n.d	0.77	2.67	1.27	1.85
Pyrene (Pyr)	n.d	n.d	1.58	0.77	3.09	n.d	n.d	0.67	n.d	n.d	2.46	n.d	1.13
Chrysene (Cry)	n.d	n.d	0.24	n.d	0.37	n.d	n.d	n.d	0.17	n.d	0.35	0.77	0.20

n.d. indicates not detected. S_{TA} is the total acidity, S_{COOH} is the carboxylic acidity, S_{OH} is the phenolic acidity, and IP is the isoelectric point.

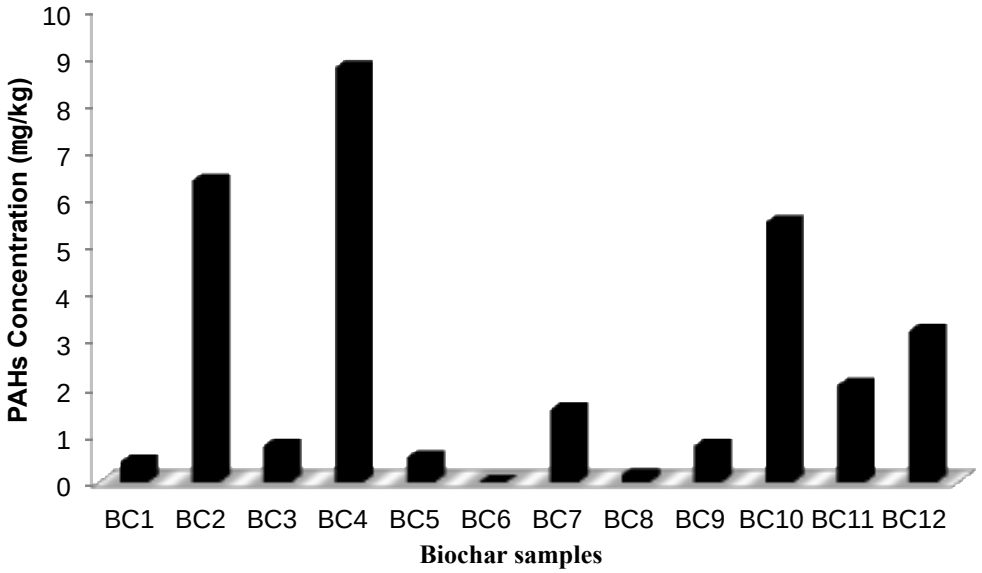

Fig. 3. Total PAHs concentration in the biochars obtained from different pyrolysis conditions

As mentioned before, the predominant compounds detected in the oat hull derived biochar were phenanthrene, pyrene, and chrysene. Nevertheless, the observed PAHs concentration in biochar was very low (0.17 to 8.73 mg/kg). The occurrence and content of each of these compounds depended on the biomass composition and chemical modification of the biomass constituents during the pyrolysis process (Anjum *et al.* 2014). Yargicoglu *et al.* (2015) reported the PAHs content in six different commercial wood-derived biochars for different production conditions. Pyrene, phenanthrene, naphthalene, fluoranthene, and acenaphthylene were found in major proportions in the biochar produced from a mixture of biomass that was 90% pine and 10% fir wood, and obtained by fast pyrolysis

The nitrogen flux and residence time of the pyrolysis of the biomass were other factors that affected the generation of PAHs during slow pyrolysis. A higher nitrogen flux reduced the chance for aromatic radicals to undergo condensation, which promoted the PAHs precursors to be conducted in the gas flux, and therefore prevented the formation of PAHs (Buss *et al.* 2016).

In the present study, the effect of nitrogen flux generated important differences in the PAHs concentrations. The experiments BC4 and BC11 had the same temperature and biomass residence time, but different nitrogen flux rates (0 L/min and 1.0 L/min, respectively), which resulted in a difference in the PAHs concentrations by about 6 µg/kg. In addition, the residence time also affected the production of PAHs. In fact, for the treatments BC4 and BC8, the final temperature was 400 °C and the nitrogen flux rate was 0 L/min, but the residence times of the biomass were 0.5 h and 3.5 h, respectively. The higher residence time showed macromolecules cracking, coupled with the generation of volatile compounds, which changed the total PAHs concentration from 8.73 µg/kg (BC4) to 0.17 µg/kg (BC8). According to Yargicoglu *et al.* (2015), the long residence times in the slow pyrolysis process generates a cracking of the PAHs formed during the first stage of pyrolysis. Therefore, these biochars can be used in agricultural applications because of their low PAHs concentrations.

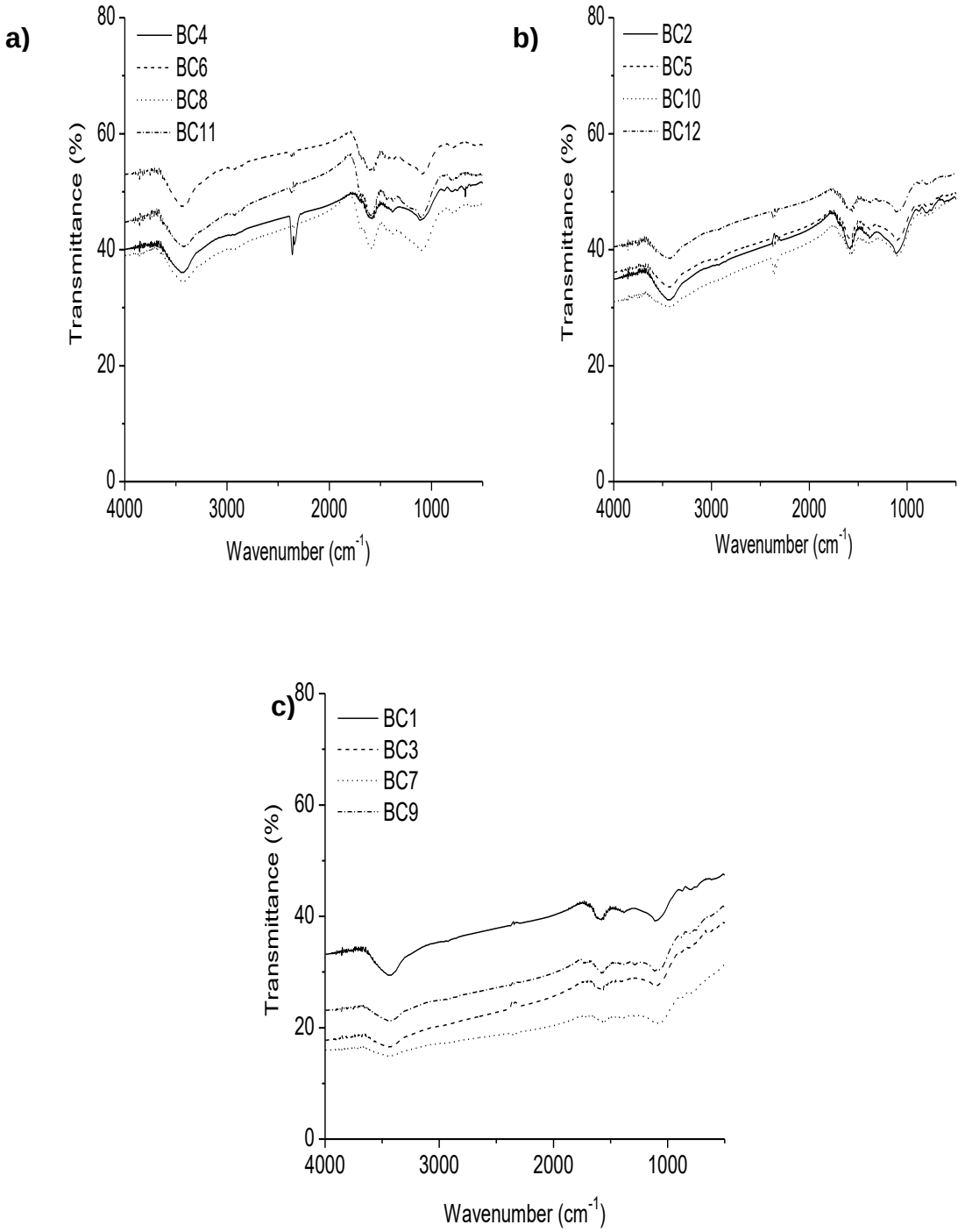

Fig. 4. FT-IR spectra of biochar from oat hull pyrolyzed at different conditions: ***a)*** synthesized at 400 °C, where **BC4**: 1.5 °C/min, 0.5 h, and 0 L/min; **BC6**: 1.5 °C/min, 3.5 h, and 1.0 L/min; **BC8**: 3.0 °C/min, 3.5 h, and 0 L/min; and **BC11**: 3.0 °C/min, 0.5 h, and 1.0 L/min; ***b)*** synthesized at 500 °C, where **BC2**: 2.25 °C/min, 2.0 h° and 0.5 L/min; **BC5**: 2.25 °C/min, 2.0 h° and 0.5 L/min; **BC10**: 2.25 °C/min, 2.0 h, and 0.5 L/min; and **BC12**: 2.25 °C/min, 2.0 h, and 0.5 L/min; and ***c)*** synthesized at 600 °C, where **BC1**: 3.0 °C/min, 0.5 h, and 0 L/min; **BC3**: 1.5 °C/min, 3.5 h, and 0 L/min; **BC7**: 3.0 °C/min, 3.5 h, and 1.0 L/min; and **BC9**: 1.5 °C/min, 0.5 h, and 1.0 L/min.

Effect of Pyrolysis Conditions on the Chemical Biochar Properties

In this study, an increase in the carbon content was observed for higher pyrolysis temperatures (Table 7). According to the literature, the increase in the total carbon content is the result of a series of reactions, such as polymerization, condensation, and aromatization. It was also observed that high pyrolysis temperatures led to increases in the pH values. According to the literature, higher pyrolysis temperatures increase the inorganic fraction (ash content) of the biochar produced (Table 7).

These results can be confirmed by observing the FT-IR spectra of the biochar samples (Fig. 4 a, b, and c). The O-H stretching band observed at approximately 3400 cm^{-1} was present in all of the biochar samples, but the intensity decreased when high pyrolysis temperatures were used. The O-H groups represent hydroxyl functional groups, supporting the results obtained for the total acidity (Table 7), which was determined mainly by the presence of alcoholic compounds. Aromatic C-C ring stretching (1590 cm^{-1} and 1400 cm^{-1}) decreased in intensity with increased temperatures. Strong bands (1200 to 1000 cm^{-1}) were assigned to the stretching of C-O of secondary alcohols. Carboxyl C-O stretching (1736 cm^{-1}) and carboxyl groups were not present in any of the samples. The surface acidity of the biochar produced at lower temperatures (400 °C) was significantly higher compared to the other biochar samples.

CONCLUSIONS

1. Different results for the biochar, bio-oil, and syngas were observed for the different pyrolysis conditions. For the operational conditions evaluated, the physicochemical characteristics of the biochar showed differences.
2. An increase in the pyrolysis temperature resulted in increases in the carbon content, pH, and specific surface area. In addition, prolonging the residence time in combination with high temperatures caused an increase in the specific surface area of the biochar.
3. The oat hull derived biochar produced under these pyrolysis conditions contained only small concentrations of PAHs, therefore, higher pyrolysis temperatures generally lead to the production of biochar with more desirable properties in the context of PAHs, and therefore, could be used in agricultural processes without any negative effects.

ACKNOWLEDGEMENTS

This work was supported by FONDECYT Projects No. 3140630, No. 1150707, and DIUFRO DI16-0138.

REFERENCES CITED

Alburquerque, J. A., Sánchez-Monedero, M. A., Roig, A., and Cayuela, M. L. (2015). "High concentrations of polycyclic aromatic hydrocarbons (naphthalene, phenanthrene and pyrene) failed to explain biochar's capacity to reduce soil nitrous

oxide emissions," *Environ. Pollut.* 196, 72-77. DOI: 10.1016/j.envpol.2014.09.014

Anjum, R., Krakat, N., Toufiq Reza, M., and Klocke, M. (2014). "Assessment of mutagenic potential of pyrolysis biochars by Ames *Salmonella*/mammalian-microsomal mutagenicity test," *Ecotox. Environ. Safe.* 107, 306-312. DOI: 10.1016/j.ecoenv.2014.06.005

Agency for Toxic Substances and Disease Registry (ATSDR) (2005). "Toxicological profile for polycyclic aromatic hydrocarbons," U. S. Department of Health and Human Services, Boca Raton, FL.

Biederman, L. A., and Harpole, W. S. (2013). "Biochar and its effects on plant productivity and nutrient cycling: A meta-analysis," *GCB Bioenergy* 5(2), 202-214. DOI: 10.1111/gcbb.12037

Buss, W., Graham, M. C., MacKinnon, G., and Maŝek, O. (2016). "Strategies for producing biochars with minimum PAH contamination," *J. Anal. Appl. Pyrol.* 119, 24-30. DOI: 10.1016/j.jaap.2016.04.001

Cetin, E., Moghtaderi, B., Gupta, R., and Wall, T. F. (2004). "Influence of pyrolysis conditions on the structure and gasification reactivity of biomass chars," *Fuel* 83(16), 2139-2150. DOI: 10.1016/j.fuel.2004.05.008

Chen, T., Zhang, Y., Wang, H., Lu, W., Zhou, Z., Zhang, Y., and Ren, L. (2014). "Influence of pyrolysis temperature on characteristics and heavy metal adsorptive performance of biochar derived from municipal sewage sludge," *Bioresource Technol.* 164, 47-54. DOI: 10.1016/j.biortech.2014.04.048

Dehkhoda, A. M., and Ellis, N. (2013). "Biochar-based catalystfor simultaneous reactions of esterification and transesterification," *Catal. Today* 207, 86-92. DOI: 10.1016/j.cattod.2012.05.034

Devi, P., and Saroha, A. K. (2015). "Effect of pyrolysis temperature on polycyclic aromatic hydrocarbons toxicity and sorption behaviour of biochars prepared by pyrolysis of paper mill effluent treatment plant sludge," *Bioresource Technol.* 192, 312-320. DOI: 10.1016/j.biortech.2015.05.084

Demirbas, A. (2004). "Effects of temperature and particle size on bio-char yield from pyrolysis of agricultural residues, " *J. Anal. Appl. Pyrolysis* 72, 243-248. DOI:10.1016/j.jaap.2004.07.003

Downie, A., Crosky, A., and Munroe, P. (2009). "Physical properties of biochar," in: *Biochar for Environmental Management Science and Technology*, J. Lehmann and S. Joseph (eds.), Earthscan, London, UK, pp. 13-32.

Fu, B., Ge, C., Yue, L., Luo, J., Feng, D., Deng, H., and Yu, H. (2016). "Characterization of biochar derived from pineapple peel waste and its application for sorption of oxytetracycline from aqueous solution," *BioResources* 11(4), 9017-9035. DOI: 10.15376/biores.11.4.9017-9035

González, M. E., Cea, M., Medina, J., González, A., Diez, M. C., Cartes, P., Monreal, C., and Navia, R. (2015). "Evaluation of biodegradable polymers as encapsulating agents for the development of a urea controlled-release fertilizer using biochar as support material," *Sci. Total Environ.* 505, 446-453. DOI: 10.1016/j.scitoenv.2014.10.014

González, M. E., Cea, M., Sangaletti, N., González, A., Toro, C., Diez, M. C., Moreno, N., Querol, X., and Navia, R. (2013). "Biochar derived from agricultural and forestry residual biomass: Characterization and potential application for enzymes immobilization," *Journal of Biobased Materials and Bioenergy* 7(6), 724-732. DOI: 10.1016/j.nbt.2012.08.167

Hale, S. E., Lehmann, J., Rutherford, D., Zimmerman, A. R., Bachmann, R. T.,

Shitumbanuma, V., O'Toole, A., Sundqvist, K. L., Arp, H. P. H., and Cornelissen, G. (2012). "Quantifying the total and bioavailable polycyclic aromatic hydrocarbons and dioxins in biochars," *Environ. Sci. Technol.* 46(5), 2830-2838. DOI: 10.1021/es203984k

Hilber, I., Blum, F., Leifeld, J., Schmidt, H. P., Bucheli, T. D. (2012). "Quantitative determination of PAHs in biochar: A prerequisite to ensure its quality and safe application," *J. Agr. Food Chem.* 60, 3042-3050. DOI: 10.1021/jf205278v

Hu, Y., Li, G., Yan, M., Ping, C., and Ren, J. (2014). "Investigation into the distribution of polycyclic aromatic hydrocarbons (PAHs) in wastewater sewage sludge and its resulting pyrolysis bio-oils," *Sci. Total Environ.* 473-474, 459-464. DOI: 10.1016/j.scitoenv.2013.12.051

Keiluweit, M., Nico, P. S., Johnson, M. G., and Kleber, M. (2010). " Dynamic molecular structure of plant biomass-derived black carbon (biochar)," *Environ. Sci. Technol.* 44(4), 1247-1253. DOI: 10.1021/es9031419

Keiluweit, M., Kleber, M., Sparrow, M. A., Simoneit, B. R. T., and Prahl, F. G. (2012). "Solvent-extractable polycyclic aromatic hydrocarbons in biochar: Influence of pyrolysis temperature and feedstock," *Environ. Sci. Technol.* 46(17), 9333-9341. DOI: 10.1021/es302125k

Khan, S., Wang, N., Reid, B. J., Freddo, A., Cai, C. (2013). "Reduced bioaccumulation of PAHs by *Lactuca satuva* L. grown in contaminated soil amended with sewage sludge and sewage sludge derived biochar," *Environ. Pollut.* 175, 64-68. DOI: 10.1016/j.envpol.2012.12.014

Keiluweit, M., Nico, P. S., Johnson, M., and Kleber, M. (2010). "Dynamic molecular structure of plant biomass-derived black carbon (biochar)," *Environ. Sci. Technol.* 44(4), 1247-1253. DOI: 10.1021/es9031419

Klasson, K. T., Uchimiya, M., and Lima, I. M. (2014). "Uncovering surface area and micropores in almond shell biochars by rainwater wash," *Chemosphere* 111, 129-134. DOI: 10.1016/j.chemosphere.2014.03.065

Lehmann, J., and Joseph, S. (2009). "Biochar for environmental management: An introduction," in: *Biochar for Environmental Management: Science and Technology*, J. Lehmann and S. Joseph (eds.), Earthscan, London, UK, pp. 1-12.

Li, J., Li, Y., Wu, Y., and Zheng, M. (2014). "A comparison of biochars from lignin, cellulose and wood as the sorbent to an aromatic pollutant," *J. Hazard. Mater.* 280, 450-457. DOI: 10.1016/j.jhazmat.2014.08.033

Manyà, J. J., Ortigosa, M. A., Laguarta, S., and Manso, J. A. (2014). "Experimental study on the effect of pyrolysis pressure, peak temperature, and particle size on the potential stability of vine shoots-derived biochar," *Fuel* 133, 163-172. DOI: 10.1016/j.fuel.2014.05.019

Novak, J. M., Lima, I., Xing, B., Gaskin, J. W., Steiner, C., Das, K. C., Ahmedna, M., Rehrah, D., Watts, D. W., Busscher, W. J., and Schomberg, H. (2009). "Characterization of designer biochar produced at different temperatures and their effects on a loamy sand," *Annals of Environmental Science* 3, 195-206.

Park, J., Hung, I., Gan, Z., Rojas, O. J., Lim, K. H., and Park, S. (2013). "Activated carbon from biochar : Influence of its physicochemical properties on the sorption characteristics of phenanthrene," *Bioresource Technol.* 149, 383-389. DOI: 10.1016/j.biortech.2013.09.085

Qin, G., Gong, D., and Fan, M. -Y. (2013). "Bioremediation of petroleum-contaminated soil by biostimulation amended with biochar," *Int. Biodeter. Biodegr.* 85, 150-155.

DOI: 10.1016/j.ibiod.2013.07.004
Qiu, Y. and Ling, F. (2006). "Role of surface functionality in the adsorption of anionic dyes on modified polymeric sorbents," *Chemosphere* 64, 963-971. DOI:10.1016/j.chemosphere.2006.01.003
Tan, K. H. (1996). *Soil Sampling, Preparation, and Analysis*, Taylor & Francis Group, Boca Raton, FL, US.
Thies, J. and Rilling, M. (2009). "Characteristics of biochar: Biological properties," in: *Biochar for Environmental Management: Science and Technology*, J. Lehmann and S. Joseph (eds.), Earthscan, London, UK, pp. 85-106.
TO-13A (1999). "Determination of polycyclic aromatic hidrocarbons (PAHs) in ambient air using gas chromatography/mass spectrometry (GC/MS)," U.S. Environmental Protection Agency, Cincinati, OH, US.
Waqas, M., Khan, S., Qing, H., Reid, B. J., and Chao, C. (2014). "The effects of sewage sludge and sewage sludge biochar on PAHs and potentially toxic element bioaccumulation in *Cucumis sativa* L.," *Chemosphere* 105, 53-61. DOI: 10.1016/j.chemosphere.2013.11.064
Yao, Y., Gao, B., Zhang, M., Inyang, M., and Zimmerman, A. R. (2012). "Effect of biochar amendment on sorption and leaching of nitrate, ammonium, and phosphate in a sandy soil," *Chemosphere* 89(11), 1467-1471. DOI: 10.1016/j.chemosphere.2012.06.002
Yargicoglu, E. N., Sadasivam, B. Y., Reddy, K. R., and Spokas, K. (2015). "Physical and chemical characterization of waste wood derived biochars," *Waste Manage*. 36, 256-268. DOI: 10.1016/j.wasman.2014.10.029

Article submitted: September 22, 2016; Peer review completed: December 12, 2016; Revised version received: January 12, 2017; Accepted: January 23, 2017; Published: February 1, 2017.
DOI: 10.15376/biores.12.1.2040-2057